

Chapter 4

**Unusual negative magnetoresistance in
 $\text{Bi}_2\text{Se}_{3-y}\text{S}_y$ Topological Insulator under
perpendicular magnetic field**

4.1: INTRODUCTION

A very interesting property observed in Bi_2Se_3 and other 3D TIs is the linear positive magneto-resistance (MR) that persists up to room temperature [60], [63], [77], [78]. Furthermore, the bulk and topological surface states (TSS) can be distinguished by Shubnikov–de Haas (SdH) oscillations and at low temperatures and high magnetic field, SdH oscillations usually superpose on the positive MR background and the π Berry phase can be extracted, which shows the transport properties of 2D Dirac fermions [45], [63], [79]–[84]. The recent interest on the unique topological properties in 3D massless Dirac fermions in “3D Dirac” or “Weyl” semimetals [85] can be revealed from the observation of an extremely large positive linear MR [86] and also the negative longitudinal MR (NLMR) when the magnetic and electric fields are co-aligned. In the present chapter, we can see that with S doping in Bi_2Se_3 the MR gradually decreases and finally it shows negative magneto-resistance (NMR) when magnetic and electric fields are perpendicular to each other which is unusual for the Topological Insulators [87].

4.2: Synthesis of Materials

The single crystal of $\text{Bi}_2(\text{Se}_{1-x}\text{S}_x)_3$ (where $x = 0, 0.02, 0.05, 0.07$). We grew it by melting a stoichiometric mixture. The mixture of high purity (99.99%) Bi, Se and S element were sealed in evacuated quartz ampule. The mixture was heated upto 900 °C at 200°C per hour and was kept at that temperature for 10 hour and then it was slowly cooled to 550°C at rate 5°C per hour. The crystal thus obtained were easily cleaved along (0,0,1) direction.

4.3: RESULT AND DISCUSSION

4.3.1: Hall Analysis

Figure 4.1 shows the variation of Hall resistivity (also the mobility (μ) and carrier concentration (n) obtained from it) with magnetic fields for $\text{Bi}_2\text{Se}_{3-y}\text{S}_y$. It is observed that carrier density for doped and undoped samples increases with temperature. In fact, at high temperature bulk contribution dominates over surface contribution and moreover, appearance of topological surface state is a complete quantum phenomenon and as a consequence, at very low temperature surface state dominates over bulk state and that is why the carrier concentration is low at low temperature.

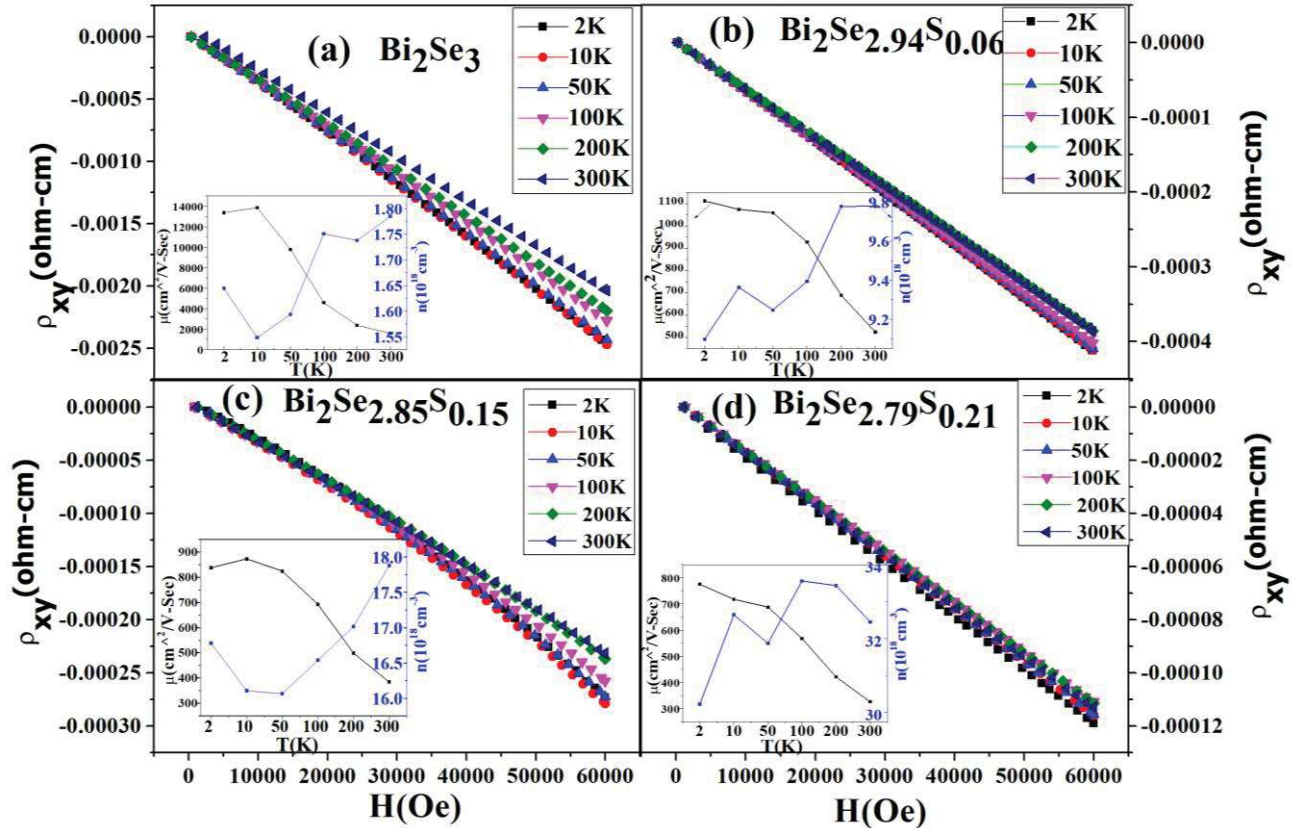


Figure 4.1: Hall resistivity as a function of magnetic field for $\text{Bi}_2\text{Se}_{3-y}\text{S}_y$. Insets: Temperature variations of carrier concentration and Hall mobility.

4.3.2: Electrical Resistivity

Figure 4.2(a) shows the resistivity as a function of temperature of $\text{Bi}_2\text{Se}_{3-y}\text{S}_y$ samples. It is observed that with increase of the S concentration, the resistivity decreases gradually which might be due to the enhanced carrier concentration, as each Se vacancy donates two inherent electrons. It is also observed that with low S doping, the resistivity at low temperature remains larger than that of the undoped sample and it decreases further with further doping of S and finally for $y=0.30$ sample the resistivity for the whole range of temperature becomes lower than that of the undoped one. The origin of this behavior we have discussed later.

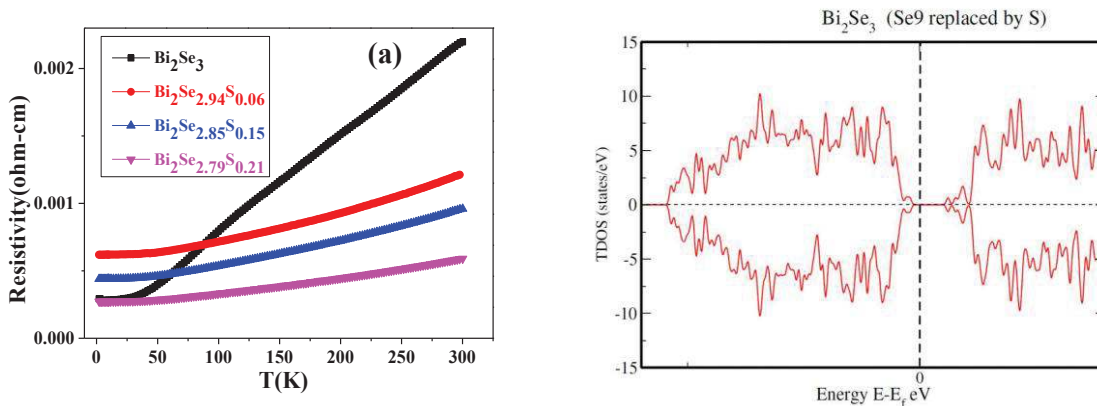


Figure 4.2: (a) Resistivity as function of temperature of $\text{Bi}_2\text{Se}_{3-y}\text{S}_y$. (b) Total DOS of S doped Bi_2Se_3 . Vertical line marks the Fermi energy.

4.3.3: Magnetoresistance Analysis

The magneto-resistance ($\text{MR} = [\rho(H) - \rho(0)] / \rho(0) \times 100\%$) of $\text{Bi}_2\text{Se}_{3-y}\text{S}_y$ as a function of magnetic field at different temperatures are shown in Figure 4.3. We have applied the magnetic field along the perpendicular direction of the plane of the sample. Bi_2Se_3 shows a large linear MR ($\sim 200\%$) at low temperature but when we increase the concentration of S its value decreases down to 7% (Figure 4.3(c)), which might be the result of increment of carrier concentration. Moreover, a negative magneto-resistance ($\sim 1\%$) is observed for $y=0.21$ sample. Interestingly, for $y=0.30$ the positive MR reappears. Furthermore, it is observed that at lower field MR shows a

quadratic behavior and then transforms to linear variation with magnetic field without saturation. The linear and quadratic MR can be represented as: $MR=aH+bH^2$ [The a and b parameters are shown in Figure 4.2(a)]. It is observed that as the temperature increases, a decreases but b increases at low temperature. Moreover it is also observed that as the doping concentration increases both a and b increase. The quadratic growth can be ascribed to a semiclassical model that conduction electron drift in a magnetic field and are deflected by Lorentz force.

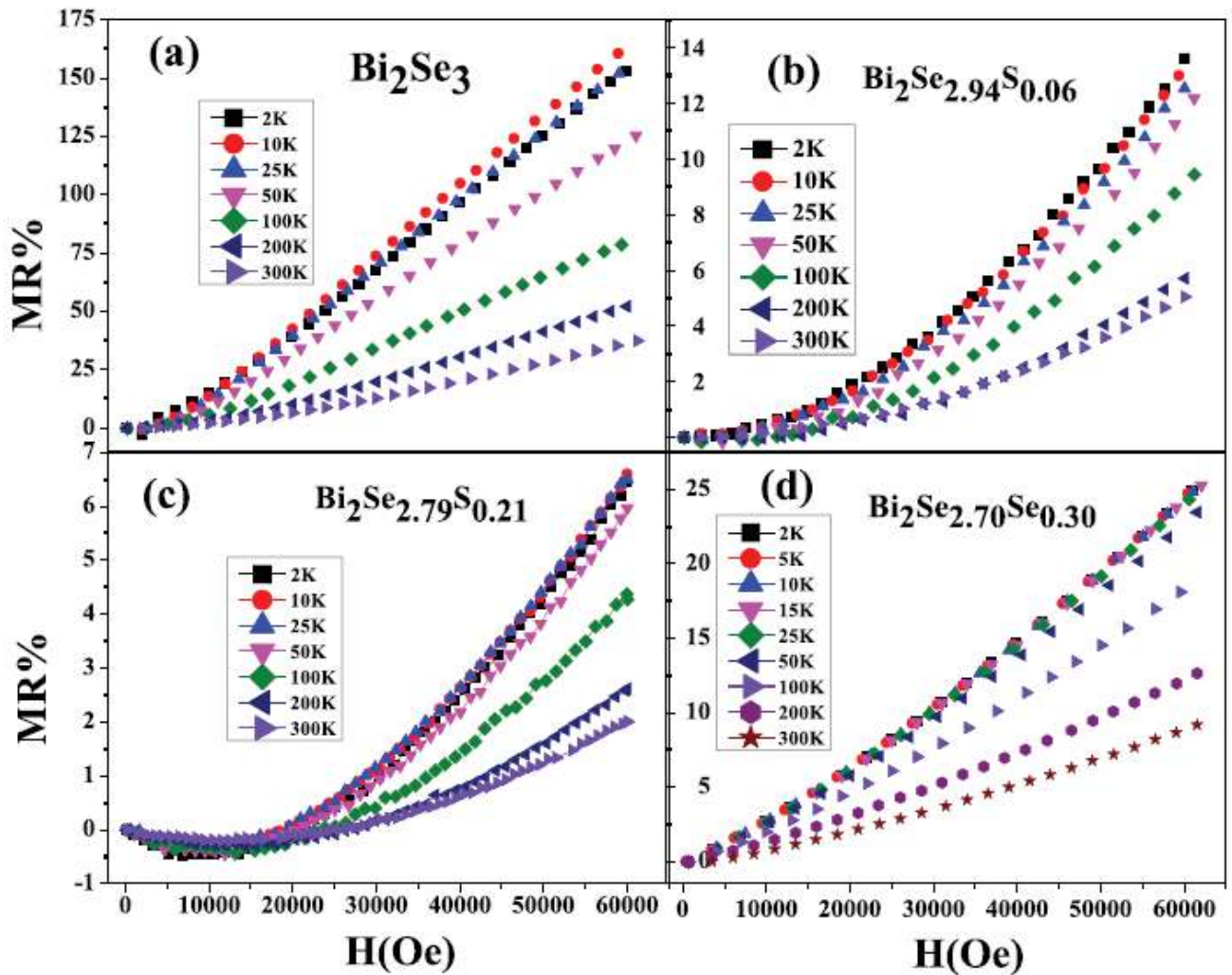


Figure 4.3: MR of Bi₂Se_{3-y}S_y as function of magnetic field at different temperatures. We have not shown here the resistivity of y=0.15 sample which shows consistent and similar behavior.

4.3.4: Shubnikov–de Haas (SdH) oscillations and Landau-level fan diagram

For a high magnetic field, Landau-level induced SdH oscillations were observed at low temperatures. Quantum oscillations are clearly visible in the second derivative $-d^2\rho_{xx}/dB^2$, as a function of the inverse field (Figure 4.4). From the fast Fourier transforms (FFTs) it is clear that three frequencies are observed. Among three frequencies one is for bulk and two are for the surface states. Taking the Onsager relation, $A(E_F)=4\pi^2e/hF$ (F is the frequency) we have calculated the n_{bulk} for the bulk band with the lowest frequency. All the bulk and surface carrier densities are shown in Table 1. Thus obtained total carrier concentrations (n_{totSdH} , given in Table 1) are in excellent agreement with n_{Hall} and also consistent with those already reported.

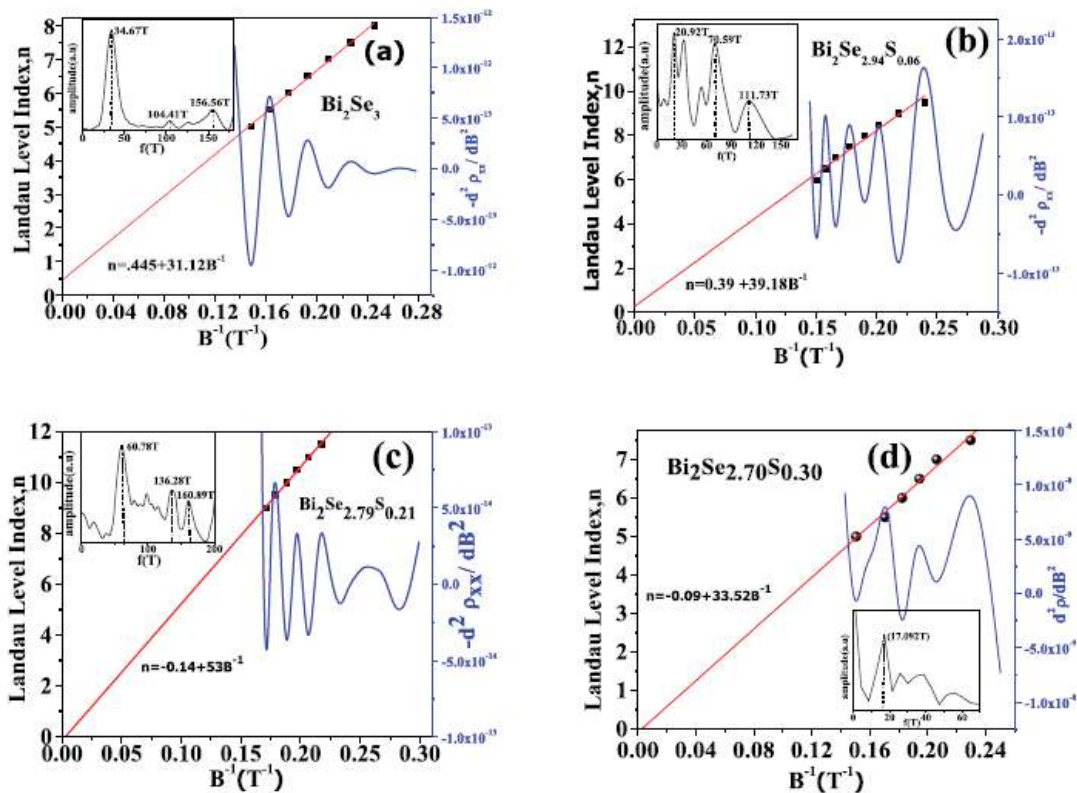


Figure 4.4: SdH oscillation and Landau level index of $\text{Bi}_2\text{Se}_{3-y}\text{S}_y$ (with $y=0, 0.06, 0.21, 0.30$) shown from $-d^2\rho_{xx}/dB^2$ as function of inverse magnetic field. Insets: Fast Fourier transform of the SdH oscillations.

The slope obtained from Landau-level fan diagram (Figure 4.4) reflects a 2D electron density, $n = (e/h) BF$. Additionally, the Landau level fan diagram shows an intercept at ~ 0.5 for the undoped sample, indicating that the Dirac fermions dominate the transport properties due to the additional Berry phase π . It is found that as the S content increases the deviation of the intercept from 0.5 also increases revealing that in the transport properties the contribution of Dirac fermion decreases, while the contribution of normal fermion increases [88]. This clearly indicates that bulk conduction gradually dominates over surface conduction with S doping. Furthermore, for $y=0.30$ obtained intersection is -0.08 which is close to zero indicating the change-over of TSS to the classical 2D electron gas. This change-over in effect suppresses the non-trivial bulk state. Similar suppression of non-trivial bulk state is also observed in Cr doped Bi_2Se_3 [89].

The observed negative magnetoresistance (NMR) in the $y=0.21$ sample is unusual. But the transition from positive to negative magnetoresistance is systematic. Generally, the NMR in TIs is observed when applied magnetic field is parallel to the electric current [90]. In the present investigation the NMR is found when the magnetic field is perpendicular to the electric current. The three possible reasons, *viz.*, Kondo effect quenching [91], [92] existence of ferromagnetic metallic state and chiral anomaly [93]–[95] are not the origin of the observed NMR in the present case. The last one is expected to be observed only in the longitudinal configuration that is when magnetic field is parallel to the electric current. However, in the present investigation the magnetic field is perpendicular to the electric current. Moreover, NMR was also found in other Anderson localized electron systems [96] which is inconsistent with the metallic regime here. So far, most of the reported NMR effects found in 3D TIs without magnetic doping are due to the weak localization (WL) effect coexisting with the weak anti localization effect under a low

magnetic field [72]. However, in the present investigation NMR cannot be due to WL effect as it shows weak temperature dependence in a wide range from 2 K to 20 K, which is not consistent as phase coherence length should be sensitive to temperature. Furthermore, the WL induced NMR will saturate on increasing the magnetic field to ~ 1 T as the magnetic length is smaller than the phase coherence length in these topological insulators [97], [98] However, our observed MR does not saturate even for the magnetic field more than 3T. Moreover, the NMR persists until 200K, far away from the point at which a weak localization effect can exist. Furthermore, in a recent paper [99] it is proposed that the observed NMR might be due to the Zeeman splitting where the rotational symmetry breaking of the Fermi circle results in the unequal density of spin-up ($D\uparrow$) and spin-down ($D\downarrow$) surface electrons. But we have carried out the DFT calculation (Figure 4.4(b)) in S doped Bi_2Se_3 and no asymmetry is observed. As a matter of fact, no local magnetic moment with S doping exists.

Recently, Breunig et al. have reported the NMR under perpendicular magnetic field in $\text{TlBi}_{2-x}\text{Sb}_x\text{Te}_{3-y}\text{Se}_y$ topological insulator and proposed it is due to the electron puddles [100]. In the present case also there is a possibility of generation of charge puddles due to the effect of doping [101]. To further confirm it we also estimated the N_{eff} from $N_{\text{eff}}=n(m_0/m^*)$ [N_{eff} is the effective no. of electrons, n is the carrier density, m_0 is the free electronic mass and m^* is the effective mass of the electron]. We determined m^* from the SdH oscillation using Onsager's relation. We observed (not shown) the N_{eff} decreases with decrease of temperature (to the lowest temperature 2K of our measurement). But if puddles are formed then at very low temperature (below a certain temperature) N_{eff} should increase with decrease of temperature and these do not contribute in dc-conduction [102].

Table 4.1: Surface and bulk Carrier concentration of $\text{Bi}_2\text{Se}_{3-y}\text{S}_y$ (with $y= 0, 0.06, 0.15, 0.21$) estimated from SdH oscillation

	$n_b(\text{cm}^{-3})$	$n_s(\text{cm}^{-2})$	$n_s(\text{cm}^{-2})$	$n_s(\text{cm}^{-2})$	$n_{\text{total}}(\text{cm}^{-3})$
Bi_2Se_3	1.1514 e+18 @34.67T	2.5197e+18@104.41T	3.7778 e+17 @156.56T		1.1518 e+18
$\text{Bi}_2\text{Se}_{2.94}\text{S}_{0.06}$	5.3969e+17 @20.92T	1.7016 e+12 @70.59T	2.6964 e+12 @111.73T		5.3990 e+17
$\text{Bi}_2\text{Se}_{2.85}\text{S}_{0.15}$	1.3442e+18 @38.44T	1.5742 e+12 @65.23T	2.5098 e+12 @104T	3.6129 e+12 149.71T	1.3446 e+18
$\text{Bi}_2\text{Se}_{2.79}\text{S}_{0.21}$	2.6726e+18 @60.78T	3.2888 e+12 @136.28T	3.8827 e+12 @160.89T		2.6731 e+18

4.3.5: S. Hikami, A. I. Larkin, and Y. O. Nagaoka (HLN) Fitting

It is clear from the Hall effect data that the Fermi level is located at the bulk conduction band due to the inevitable n -type doping from Se vacancies [24] which means that the bulk conduction electrons and the surface states can coexist to contribute to the conductance. Therefore, the bulk origin may play a dominant role in the NMR as it is observed under a perpendicular magnetic field, which is consistent with the three dimensional bulk conduction channels. To further support this we have fitted the MR data with the HLN formula [103] According to the HLN formula, magneto-conductance can be expressed as

$$\sigma(B) = -A [\Psi(1/2 + \hbar/4el_\phi^2 B) - \ln(\hbar/4el_\phi^2)] \quad (4.1)$$

Where ψ is the digamma function, l_ϕ is the phase coherence length, the distance travelled by an electron with a constant phase. A is related to the number of conduction channel, $A = \alpha(e^2/2\pi^2\hbar)$ with $\alpha=1/2$ per conduction channel. We have fitted our experimental data (Figure 4.5(a)) in the low field range (0 to 1T) with the above equation for $\text{Bi}_2\text{Se}_{3-y}\text{S}_y$ (with $y= 0, 0.06, 0.15, 0.21$) and the fitted parameters A and l_ϕ are determined. In Figure 4.5 we have also represented the number of channels (determined from the value of A) as function of temperature. The number of channels

is five times more than those found in two-dimensional systems and the values are consistent with those reported for single crystals [73].

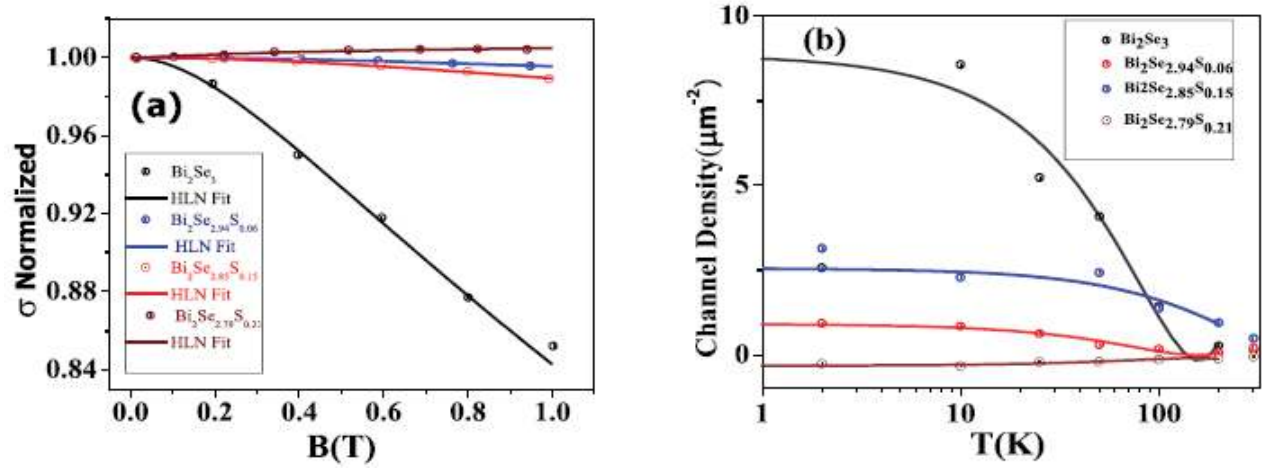


Figure 4.5: (a) Fitting of conductivity as function of magnetic field of $\text{Bi}_2\text{Se}_{3-y}\text{S}_y$ with HLN model. (b) Channel density of $\text{Bi}_2\text{Se}_{3-y}\text{S}_y$ as a function of temperature estimated from HLN model fitting.

The change of number of channels with S doping is also consistent with the resistivity behavior. It is observed in $y=0.06$ sample the number of channels decrease but as the doping concentration increases to $y=0.15$ the number of channels increase but still lower than those of the undoped sample. With further increase of doping concentration to $y=0.21$ interestingly surface channel density decreases. We have observed in low temperature resistivity data (Figure 4.2) that initially conductivity decreases for $y=0.06$ sample and for $y=0.15$ the conductivity becomes higher than that of the $y=0.06$ sample but remains lower compared to undoped sample. Furthermore, for $y=0.21$, maximum conductivity is observed which is larger than that of the undoped sample. The enhancement of conductivity and decrement of surface channel density can be explained by the increment of number of bulk channels. Therefore, it confirms that the NMR is due to the bulk conduction. But for $y=0.30$ the non-trivial bulk state is destroyed and the positive MR reappears. Therefore, the negative MR is due to non-trivial bulk state. It is worthwhile to mention that though initially with S doping the resistivity at relatively higher temperature decreases, but at lower temperature ($<100\text{K}$) it remains larger than that of the

undoped sample. This might also be due to the dominance of bulk contribution with S doping. As we have already mentioned (from Hall data) that at higher temperature surface contribution gradually decreases, therefore, with increase of S doping the temperature span of the decrease of resistivity gradually increases.

Moreover, this is to further mention that the origin of NMR might be the inhomogeneous distribution or the cluster formation of S. But if this is the origin then for $y=0.3$ sample we should also get the negative magneto resistance. However, it deserves further study to throw more light on the origin of the negative MR in this S doped Bi_2Se_3 .

4.8: CONCLUSION

In conclusion, we have investigated the magnetotransport properties of $\text{Bi}_2\text{Se}_{3-y}\text{S}_y$. All the samples show the metallic behavior throughout the whole temperature range. Initially, at lower temperature, the resistivity is greater than that of the undoped sample for $y=0.06$ and 0.15 . But as the S content increases, the resistivity decreases, and finally, for the $y=0.21$ sample, the resistivity becomes the lowest throughout the whole temperature range of measurement. The MR also decreases with an increase in the S content, and finally, for the $y=0.21$ sample, it becomes negative. All the samples show SdH oscillations in $d^2\rho_{xx}/dB^2$ as a function of inverse magnetic field curves. The fast Fourier transform of SdH oscillation shows the existence of both surface and bulk states. The NMR of the $y=0.21$ sample has been explained as the dominance of the non-trivial bulk conduction over surface conduction. Furthermore, with a further increase in the S content ($y=0.30$), the non-trivial bulk state is destroyed.